CD4+ T cells support glial neuroprotection, slow disease progression, and modify glial morphology in an animal model of inherited ALS

David R. Beers*, Jenny S. Henkel*, Weihua Zhao, Jinghong Wang, and Stanley H. Appel†

Department of Neurology, Methodist Neurological Institute, Houston, TX

Neuroinflammation, marked by gliosis and infiltrating T cells, is a prominent pathological feature in diverse models of dominantly inherited neurodegenerative diseases. Recent evidence derived from transgenic mice ubiquitously overexpressing mutant Cu^{2+}/Zn^{2+} superoxide dismutase (mSOD1), a chronic neurodegenerative model of inherited amyotrophic lateral sclerosis (ALS), indicates that glia with either a lack of or reduction in mSOD1 expression enhance motoneuron protection and slow disease progression. However, the contribution of T cells that are present at sites of motoneuron injury in mSOD1 transgenic mice is not known. Here we show that when mSOD1 mice were bred with mice lacking functional T cells or CD4+ T cells, motoneuron disease was accelerated, accompanied by unexpected attenuated morphological markers of gliosis, increased mRNA levels for proinflammatory cytokines and NOX2, and decreased levels of trophic factors and glial glutamate transporters. Bone marrow transplants reconstituted mice with T cells, prolonged survival, suppressed cytotoxicity, and restored glial activation. These results demonstrate for the first time in a model of chronic neurodegeneration that morphological activation of microglia and astroglia does not predict glial function, and that the presence of CD4+ T cells provides supportive neuroprotection by modulating the trophic/cytotoxic balance of glia. These glial/T-cell interactions establish a novel target for therapeutic intervention in ALS and possibly other neurodegenerative diseases.

amyotrophic lateral sclerosis | astrocytes | bone marrow transplant | microglia | superoxide dismutase

Dysfunction or death of specific neuronal populations most at risk for dominantly inherited neurodegenerative diseases is not mediated solely by the expression of the mutant protein within target neurons (1). Dominant mutations in the Cu^{2+}/Zn^{2+} superoxide dismutase (mSOD1) gene are the most frequent cause of inherited amyotrophic lateral sclerosis (ALS), an inexorably progressive and fatal neuromuscular disease, and current evidence suggests that motoneuron injury is non−cell-autonomous and involves damage caused by mSOD1 proteins within glia of the central nervous system (CNS) (1−4). Reduced mSOD1 protein levels in astroglia have been shown to delay microglial activation and to sharply slow disease progression (5). Eliminating or reducing mSOD1 expression from microglia also slows motoneuron loss and disease progression (6, 7). Although neuroinflammation is a pathological hallmark in transgenic mice ubiquitously overexpressing mSOD1 (8, 9), the role of T cells in this model of chronic neurodegeneration is not understood; however, they have been shown to modulate microglial activation and provide neuroprotection in acute models of neuronal injury (10−16). Thus, to assess the role of T cells in a chronic neurodegenerative disease such as ALS, immunodeficient mice were bred with mSOD1^{G93A} transgenic mice and selective reconstitution experiments with bone marrow transplants (BMT) were used to elucidate the roles of T cells. These studies provide compelling evidence that the presence of CD4+ T cells, either directly or indirectly, morphologically and functionally alter microglial and astroglial activation, and may support neuro-protection by modulating the glial balance between trophism and cytotoxicity.

Results

CCR2$^{-/-}$ Donor Cells Are Not Neuroprotective. To examine possible contributions of the peripheral immune system on disease progression, mSOD1^{G93A}/PU.1$^{-/-}$ mice on a B6/SJL genetic background [supporting information (SI)] received BMT from CCR2$^{-/-}$ mice lacking the receptor for monocyte-chemoattractant protein−1 (MCP-1/CCL2) (6). MCP-1 recruits CCR2-expressing cells, including activated T cells and monocytes, to sites of injury (17, 18) and is increased in mSOD1^{G93A} mice (19). Although mean onset times were not different between groups (SI Text, Fig. S1), mSOD1^{G93A}/PU.1$^{-/-}$ mice receiving CCR2$^{-/-}$ BMT had shorter life spans and disease durations than mSOD1^{G93A}/PU.1$^{-/-}$ mice transplanted with wild-type (WT) bone marrow (survival, $P = 0.026$; duration, $P = 0.032$), similar to mSOD1^{G93A}/PU.1$^{-/-}$ mice transplanted with mSOD1^{G93A} bone marrow and mSOD1^{G93A}/PU.1$^{+/-}$ littermates (Fig. 1 A and B). With the exception of expressing CCR2, the engrafted microglia were WT and yet demonstrated less immunohistochemical evidence of morphological activation than mice transplanted with WT bone marrow (Fig. 1C and D). Unlike mSOD1^{G93A}/PU.1$^{-/-}$ mice that received mSOD1^{G93A} or WT BMT, CD3+ T cells were not observed in mSOD1^{G93A}/PU.1$^{-/-}$ mice with CCR2$^{-/-}$ BMT (Fig. 1 E and F).

T and/or B Cells Contribute to Neuroprotection. The significance of infiltrating lymphocytes were assayed by breeding mSOD1^{G93A} mice with recombination-activating gene 2 knockout (RAG2$^{-/-}$) mice that lack functional T and B cells (20). Although onset times were not different (Fig. S2), mSOD1^{G93A}/RAG2$^{-/-}$ mice on a C57BL/6 genetic background (SI Text) had shorter life spans and disease durations than mSOD1^{G93A}/RAG2$^{+/-}$ littermates (mean survival, $P = 0.00001$; duration, $P = 0.00001$) (Fig. 1G and H), suggesting T and/or B cells contribute to neuroprotection. To determine whether RAG2 has unknown CNS functions, sublethally γ-irradiated mSOD1^{G93A}/RAG2$^{-/-}$ mice were reconstituted with functional T and B cells by BMT from either mSOD1^{G93A} or WT mice. Transplanted mSOD1^{G93A}/RAG2$^{-/-}$ mice survived longer with a slower disease progression than non-transplanted mSOD1^{G93A}/RAG2$^{-/-}$ mice (mSOD1^{G93A}: survival, $P = 0.00004$ and duration, $P = 0.0016$; WT: survival, $P = 0.001$ and duration, $P = 0.0025$), similar to mSOD1^{G93A}/RAG2$^{+/-}$ mice (Fig. 1G and
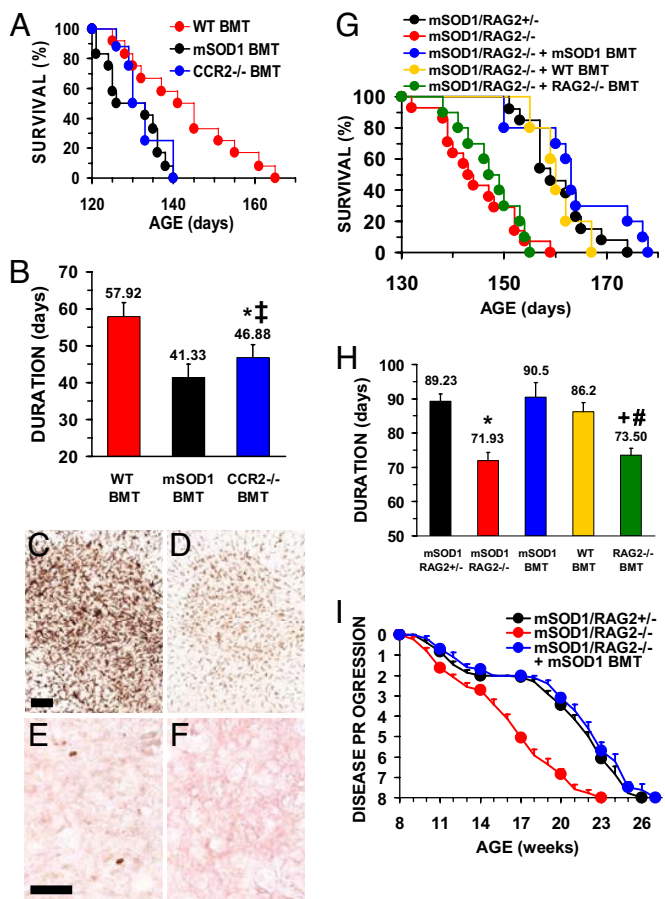
Fig. 1. T cells prolong survival. (*A*) mSOD1^{G93A}/PU.1$^{-/-}$ mice on a B6/SJL genetic background receiving CCR2$^{-/-}$ BMT have a shorter survival time (133 ± 2 days, *n* = 10) than mSOD1^{G93A}/PU.1$^{-/-}$ mice after WT BMT (141 ± 3 days, *n* = 12), and were similar to mSOD1^{G93A}/PU.1$^{+/-}$ littermates (133 ± 2 days, *n* = 12; data not shown for clarity) and mSOD1^{G93A}/PU.1$^{-/-}$ mice with mSOD1^{G93A} BMT (130 ± 2 days, *n* = 12). (*B*) Disease duration was attenuated in mSOD1^{G93A}/PU.1$^{-/-}$ mice receiving CCR2$^{-/-}$ BMT. Data for mSOD1^{G93A}/PU.1$^{+/-}$ mice were eliminated for clarity but were similar to mSOD1^{G93A}/PU.1$^{-/-}$ mice with mSOD1^{G93A} BMT (*P* = 0.55). (*C*) CD11b immunohistochemistry of morphologically activated microglia at end-stage disease in mSOD1^{G93A}/PU.1$^{+/-}$ mice. (*D*) Following BMT with CCR2$^{-/-}$ donor-derived cells, the CD11b signal from microglia of mSOD1^{G93A}/PU.1$^{-/-}$ was reduced. (*E*) CD3+ T cells were observed in mSOD1^{G93A}/PU.1$^{+/-}$ mice. (*F*) CD3+ T cells were absent in mSOD1^{G93A}/PU.1$^{-/-}$ mice receiving CCR2$^{-/-}$ BMT. (*G*) Survival times were shorter in mSOD1^{G93A}/RAG2$^{-/-}$ mice, on a C57BL/6 genetic background, lacking functional T and B cells (145 ± 2 days, *n* = 14) than in mSOD1^{G93A}/RAG2$^{+/-}$ littermates (161 ± 2 days, *n* = 13), but were prolonged following BMT (mSOD1^{G93A}: 164 ± 3 days, *n* = 10; WT: 161 ± 2 days, *n* = 10). RAG2$^{-/-}$ BMT did not increase survival (148 ± 2 days, *n* = 10). Survival of mSOD1^{G93A}/RAG2$^{+/-}$ mice were similar to mSOD1^{G93A}/RAG2$^{+/+}$ (160 ± 3 days, *n* = 20, *P* = 0.61). (*H*) Disease duration was shorter in mSOD1^{G93A}/RAG2$^{-/-}$ mice than mSOD1^{G93A}/RAG2$^{+/-}$ littermates, but was prolonged following BMT. (*I*) Disease progression in mSOD1^{G93A}/RAG2$^{-/-}$ mice lacked the 4-week plateau of mSOD1^{G93A}/RAG2$^{+/-}$ mice and was re-established after mSOD1^{G93A} BMT. *, Not different from mSOD1^{G93A}/PU.1$^{-/-}$ mice with mSOD1^{G93A} BMT; ‡different from mSOD1^{G93A}/PU.1$^{-/-}$ mice with WT BMT; +different from mSOD^{G93A}/RAG2$^{+/-}$; #, not different from mSOD^{G93A}/RAG2$^{-/-}$. (Scale bars: *C* and *D*, 100 μm; *E* and *F*, 50 μm.)

H, and Fig. S2). Because lethal γ-irradiation with 1100 cGy may artificially induce circulating myeloid cells to infiltrate the CNS (21, 22), the mice in this study received sublethal 400 cGy γ-irradiation treatments. This dose of γ-irradiation did not induce additional myeloid cell infiltration into the CNS (data not shown). However, to ensure that the increased survival was not caused by additional
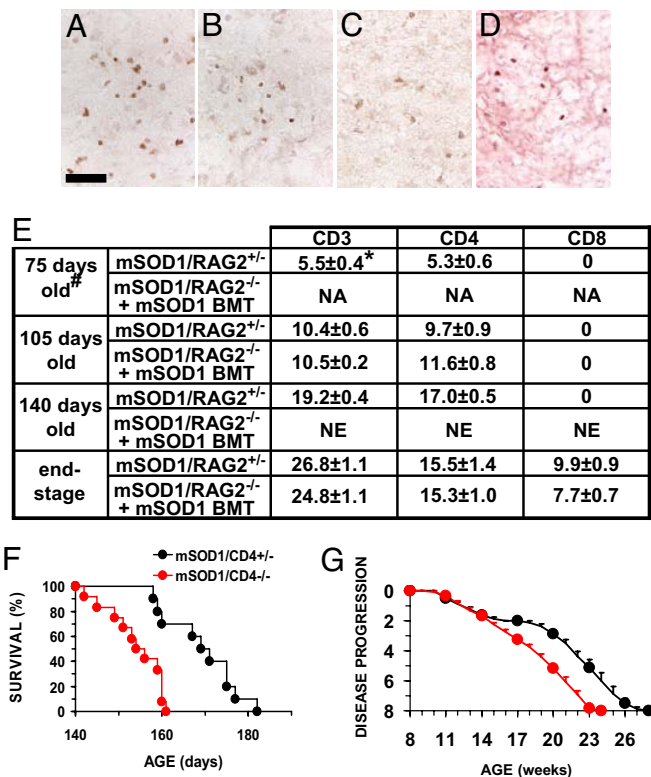

		CD3	CD4	CD8
75 days old [#]	mSOD1/RAG2$^{+/-}$	5.5±0.4*	5.3±0.6	0
	mSOD1/RAG2$^{-/-}$ + mSOD1 BMT	NA	NA	NA
105 days old	mSOD1/RAG2$^{+/-}$	10.4±0.6	9.7±0.9	0
	mSOD1/RAG2$^{-/-}$ + mSOD1 BMT	10.5±0.2	11.6±0.8	0
140 days old	mSOD1/RAG2$^{+/-}$	19.2±0.4	17.0±0.5	0
	mSOD1/RAG2$^{-/-}$ + mSOD1 BMT	NE	NE	NE
end-stage	mSOD1/RAG2$^{+/-}$	26.8±1.1	15.5±1.4	9.9±0.9
	mSOD1/RAG2$^{-/-}$ + mSOD1 BMT	24.8±1.1	15.3±1.0	7.7±0.7

Fig. 2. Immunohistochemical evaluations revealed the presence of T cells. CD3+ T cells were documented at end-stage disease in mSOD1^{G93A}/RAG2$^{+/-}$ mice (*A*) and were observed in mSOD1^{G93A}/RAG2$^{-/-}$ mice following mSOD1^{G93A} BMT (*B*). Similar results were obtained using antibodies to CD4 (*C*). Only CD8+ T cells were observed in mSOD1^{G93A}/CD4$^{-/-}$ mice (*D*). Numbers and subpopulations of T cells in lumbar spinal cords (*E*). mSOD1^{G93A}/CD4$^{+/-}$ mice survived longer (170 ± 3 days, *n* = 10) than mSOD1^{G93A}/CD4$^{-/-}$ mice (154 ± 2 days, *n* = 12), both on C57BL/6 genetic backgrounds (*F*). There was a 4-week plateau in mSOD1^{G93A}/CD4$^{+/-}$ mice that was absent in mSOD1^{G93A}/CD4$^{-/-}$ mice (*G*). #, *n* = 3 for each time point. *, Mean number of cells per 30-μm section ± SEM. NA, not appropriate (just after BMT); NE, not examined. (Scale bar: 50 μm.)

leukocytes and the radiation treatment, sublethally γ-irradiated mSOD1^{G93A}/RAG2$^{-/-}$ mice received BMT from RAG2$^{-/-}$ mice that have normal functioning monocytes/macrophages, neutrophils, etc (20). Survival times of mSOD1^{G93A}/RAG2$^{-/-}$ mice receiving RAG2$^{-/-}$ BMT were similar to non-transplanted mSOD1^{G93A}/RAG2$^{-/-}$ mice, but shorter survival times and disease durations than mSOD1^{G93A}/RAG2$^{-/-}$ mice transplanted with either mSOD1^{G93A} or WT bone marrows (mSOD1^{G93A}: survival, *P* = 0.0001 and duration, *P* = 0.003; WT: survival, *P* = 0.001 and duration, *P* = 0.005) (Fig. 1*G* and *H*, and Fig. S2).

T and/or B Cells Influence the Rate of Disease Progression. Rates of disease progression (6) were different at 11 weeks of age when mSOD1^{G93A}/RAG2$^{-/-}$ mice were compared with mSOD1^{G93A}/RAG2$^{+/-}$ mice (*P* = 0.0006) and further diverged between 14 and 18 weeks, a time at which disease progression plateaued in mSOD1^{G93A}/RAG2$^{+/-}$ mice (Fig. 1*I*) (23). Following BMT with mSOD1^{G93A} cells, mSOD1^{G93A}/RAG2$^{-/-}$ mice had a similar 4 week latency progression profile as mSOD1^{G93A}/RAG2$^{+/-}$ mice.

Presence of T-Cells Is Restored After BMT. Using CD3, a pan T-cell marker, CD4, and CD8 antibodies, the presence of T cells were examined in lumbar spinal cords from 75 (disease onset), 105 (the plateau phase), and 140 (the declining performance phase) day old mice, and at end-stage disease (Fig. 2 *A–D* and Fig. S3*A–D*). No
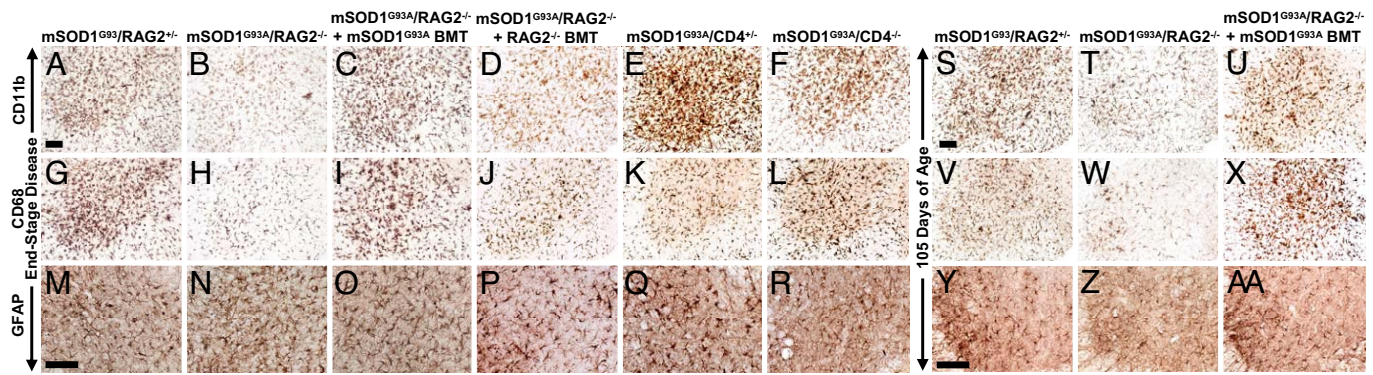
NEUROSCIENCE

Fig. 3. Immunohistochemical evaluations of lumbar spinal cord. The CD11b microglial/macrophage signal observed at end-stage disease in lumbar spinal cord sections of mSOD1^{G93A}/RAG2$^{+/-}$ mice (*A*) was decreased in mSOD1^{G93A}/RAG2$^{-/-}$ mice (*B*) and restored after mSOD1^{G93A} BMT (*C*). CD11b signal was not restored after RAG2$^{-/-}$ BMT (*D*). As with mSOD1^{G93A}/RAG2$^{-/-}$ mice, the CD11b immunoreactivity observed at end-stage disease in mSOD1^{G93A}/CD4$^{+/-}$ mice (*E*) was reduced in mSOD1^{G93A}/CD4$^{-/-}$ mice (*F*). Similar results were observed with antibodies to CD68 (*G–L*), which was consistent with the quantitative RT-PCR results. GFAP immunoreactivity was not different between groups at end-stage disease (*M–O*) and was unchanged after RAG2$^{-/-}$ BMT (*P*). The GFAP signal observed in mSOD1^{G93A}/CD4$^{+/-}$ mice (*Q*) was less in mSOD1^{G93A}/CD4$^{-/-}$ mice (*R*). Compared with that observed with CD11b staining of mSOD1^{G93A}/RAG2$^{+/-}$ mice at 105 days of age (*S*), microglial activation was less in mSOD1^{G93A}/RAG2$^{-/-}$ mice at the same age (*T*) and again restored following mSOD1^{G93A} BMT (*U*). Similar results were observed with CD68 at 105 days of age (*V–X*). Compared with mSOD1^{G93A}/RAG2$^{+/-}$ mice at 105 days of age (*Y*), astrocyte activation was reduced in mSOD1^{G93A}/RAG2$^{-/-}$ mice at 105 days of age (*Z*) and restored after mSOD1^{G93A} BMT (*AA*). (Scale bars: *A–L* and *S–X*, 100 μm; *M–R* and *Y–AA*, 100 μm.)

CD3+, CD4+, or CD8+ T cells were observed in mSOD1^{G93A}/RAG2$^{-/-}$ mice. CD3+ T cells were observed at every age examined, with increasing numbers as the disease progressed. At 75, 105, and 140 days of age, there were 6, 10, and 19 CD3+ cells per section, respectively, localized predominantly to the ventral gray matter (Fig. 2*E*). At these ages, only CD4+ cells were observed with cell numbers similar to CD3+ cells; no CD8+ cells were observed. At end-stage disease, there were 27 CD3+ cells per section. ≈60% were CD4+ with the remaining cells staining for CD8. Similar numbers and subtypes of T cells were observed in mSOD1^{G93A}/RAG2$^{-/-}$ mice following BMT with either mSOD1^{G93A} or WT donor-derived cells. Using antibodies to CD19, a B-cell marker, B cells were not present in any lumbar spinal cord section examined from 105- and 140-day-old mSOD1^{G93A}/RAG2$^{+/-}$ mice and mSOD1^{G93A}/RAG2$^{-/-}$ mice with BMT. At end-stage disease, there was no consistent convincing evidence for the presence of B cells.

Presence of CD4+ T-Cells Is Responsible for Prolonged Disease Duration and Survival. Because only CD4+ T cells were observed at all phases of disease, mSOD1^{G93A} transgenic mice were bred with CD4 knockout (CD4$^{-/-}$) mice that lack surface expression of CD4, but have unaltered myeloid-, CD8+ T and B cells (24). Although disease onset was not different (Fig. S4*A*), survival of mSOD1^{G93A}/CD4$^{-/-}$ mice was shorter than mSOD1^{G93A}/CD4$^{+/-}$ littermates ($P = 0.001$) (Fig. 2*F*) and was similar to the difference in survival times between mSOD1^{G93A}/RAG2$^{+/-}$ and mSOD1^{G93A}/RAG2$^{-/-}$ mice (15.6 days vs 15.8 days). Disease duration was also different between mSOD1^{G93A}/CD4$^{+/-}$ and mSOD1^{G93A}/CD4$^{-/-}$ littermates ($P = 0.0004$) (Fig. S4*B*) and was again analogous to mSOD1^{G93A}/RAG2$^{-/-}$ mice (17.4 vs 17.3 days). Disease progression with mSOD1^{G93A}/CD4$^{+/-}$ mice reached a plateau between 15 and 19 weeks, whereas mSOD1^{G93A}/CD4$^{-/-}$ mice continued to decline (Fig. 2*G*, $P = 0.03$ at 15 weeks and diverged further thereafter).

Morphological Markers of Glial Activation Are Attenuated in mSOD1^{G93A} Mice Lacking Functional T-Cells. Immunohistochemical evaluations of lumbar spinal cords at end-stage disease revealed less morphological activation of microglia in mSOD1^{G93A}/RAG2$^{-/-}$ mice compared with mSOD1^{G93A}/RAG2$^{+/-}$ littermates, even though their survival time was shorter (Fig. 3 *A–C* and *G–I* and Fig. S5*A–I*). Following mSOD1^{G93A} BMT, the CD11b, CD68, CD11c,

CD40, and MHC II immunoreactivities were restored in mSOD1^{G93A}/RAG2$^{-/-}$ mice and were comparable to those observed in mSOD1^{G93A}/RAG2$^{+/-}$ mice. Similar results were obtained with mSOD1^{G93A}/RAG2$^{-/-}$ mice reconstituted with WT BMT. Quantitative real-time polymerase chain reaction (RT-PCR) confirmed that there was less CD68 mRNA in mSOD1^{G93A}/RAG2$^{-/-}$ mice than mSOD1^{G93A}/RAG2$^{+/-}$ littermates ($P = 0.001$) and was restored following BMT (Fig. 4*A*). At 105 days of age, there was a reduction of CD11b (Fig. 3*S–U*) and CD68 (Fig. 3*V–X*) signal in lumbar spinal cord sections from mSOD1^{G93A}/RAG2$^{-/-}$ mice compared with mSOD1^{G93A}/RAG2$^{+/-}$ littermates. However, at 75 days of age, this distinction was not evident (Fig. S5*J–M*). To control for other leukocytes possibly influencing the status of microglial activation in these mice, transplantation of RAG2$^{-/-}$ bone marrow cells into mSOD1^{G93A}/RAG2$^{-/-}$ mice did not restore the morphological activation of microglia (Fig. 3*D* and *J*).

To address the question of whether all glial responses were reduced, astroglial morphology was evaluated in lumbar spinal cords. At end-stage disease, GFAP immunoreactivity was increased in transgenic mice compared with WT mice (Fig. 3*M–O*). This increase was confirmed using quantitative RT-PCR for GFAP (Fig. 4*B*). Furthermore, both qualitatively and quantitatively, there were no differences in the expression of GFAP between any transgenic mouse line or after BMT (Fig. 3*P*). At 105 days of age, mSOD1^{G93A}/RAG2$^{-/-}$ mice had reduced GFAP signal compared to mSOD1^{G93A}/RAG2$^{+/-}$ mice and BMT restored the GFAP immunoreactivity (Fig. 3*Y–AA*). GFAP immunoreactivity was observably less at 75 days of age in sections from mSOD1^{G93A}/RAG2$^{-/-}$ mice compared with sections from mSOD1^{G93A}/RAG2$^{+/-}$ mice (Fig. S5*N* and *O*).

Immunohistochemical evaluation of microglia in lumbar spinal cords of mSOD1^{G93A}/CD4$^{-/-}$ mice showed a similar attenuation of CD11b and CD68 signal as observed in mSOD1^{G93A}/RAG2$^{-/-}$ mice (Fig. 3*E*, *F*, *K*, and *L*). Quantitative RT-PCR confirmed that the message for CD68 in lumbar spinal cords was reduced in mSOD1^{G93A}/CD4$^{-/-}$ mice ($P = 0.03$) (Fig. 4*A*). However, unlike the astrogliosis noted at end-stage disease for mSOD1^{G93A}/RAG2$^{-/-}$ mice, there was an observable reduction in GFAP immunoreactivity in mSOD1^{G93A}/CD4$^{-/-}$ mice compared with mSOD1^{G93A}/CD4$^{+/-}$ mice (Fig. 3*Q* and *R*). Although CD4+ and CD8+ T cells were observed in mSOD1^{G93A}/CD4$^{+/-}$ mice (data

Fig. 4. Quantitative RT-PCR results (note the different ordinate for each graph). Normalized to β-actin. For all groups of mice, $n = 3$. (*A*) Quantitative RT-PCR determined that the mRNA level for CD68 is reduced in mSOD1^{G93A}/RAG2$^{-/-}$ mice and restored after mSOD1^{G93A} BMT. The mSOD1^{G93A}/CD4$^{-/-}$ mice also had reduced levels of CD68. These results are consistent with the immunohistochemical observations. (*B*) The mRNA level for GFAP was increased in all mSOD1^{G93A} groups of mice. (*C–E*) There were reduced message levels for IGF-1, GDNF, and BDNF in mSOD1^{G93A}/RAG2$^{-/-}$ mice compared with mSOD1^{G93A}/RAG2$^{+/-}$ mice at end-stage disease, and the levels were restored after mSOD1^{G93A} BMT. Message levels for these neurotrophic factors were also reduced in mSOD1^{G93A}/CD4$^{-/-}$ mice. Similar results were obtained for GLT-1 (*F*) and GLAST (*G*), glutamate transporters predominately localized on astrocytes. (*H*) IL-4 was reduced in mSOD1^{G93A}/RAG2$^{-/-}$ mice compared with mSOD1^{G93A}/RAG2$^{+/-}$ mice, but was restored following mSOD1^{G93A} BMT. mSOD1^{G93A}/CD4$^{-/-}$ mice also had a reduced mRNA level for IL-4. (*I*) TGF-β, an anti-inflammatory/neurotrophic factor, was decreased in mSOD1^{G93A}/RAG2$^{-/-}$ mice compared with mSOD1^{G93A}/RAG2$^{+/-}$ mice but was again restored following mSOD1^{G93A} BMT. (*J*) In contrast to IL-4 and TGF-β, the proinflammatory agent TNF-α was elevated in mSOD1^{G93A}/RAG2$^{-/-}$ and mSOD1^{G93A}/CD4$^{-/-}$ mice. (*K*) NOX2, a subunit in the enzyme responsible for the production of highly toxic superoxide molecules, was also elevated in mSOD1^{G93A}/RAG2$^{-/-}$ and mSOD1^{G93A}/CD4$^{-/-}$ mice. +, increased compared with WT mice, $P < 0.05$; *, decreased compared with mSOD1^{G93A} or mSOD1^{G93A}/RAG2$^{+/-}$ mice, $P < 0.05$; ‡, not different from mSOD1^{G93A}/RAG2$^{-/-}$ mice; #, not different from mSOD1^{G93A}/RAG2$^{+/-}$ mice; **, increased compared with mSOD1^{G93A} or mSOD1^{G93A}/RAG2$^{+/-}$ mice, $P < 0.05$; ##, decreased compared with mSOD1^{G93A}/RAG2$^{-/-}$ mice, $P < 0.05$.
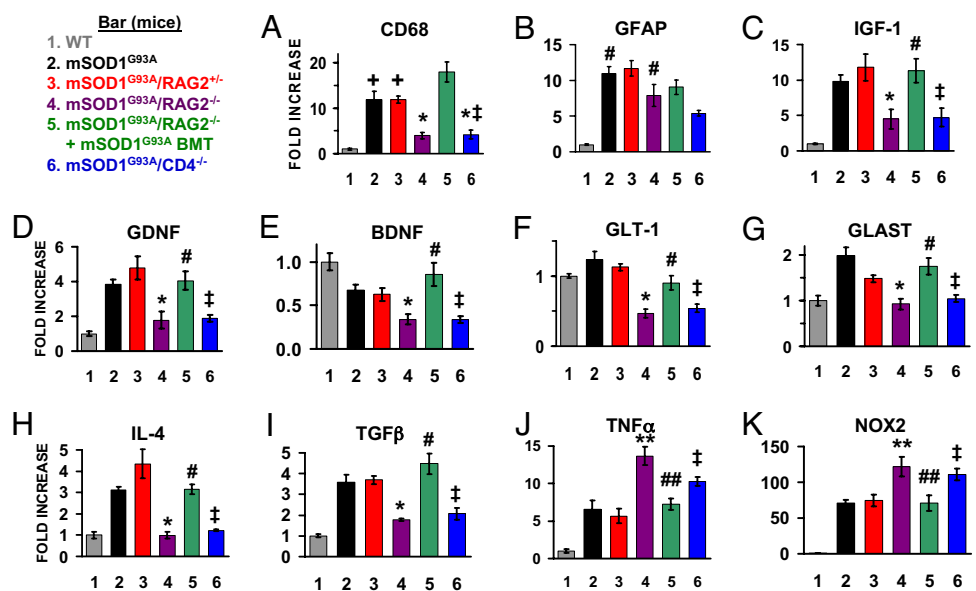
not shown), CD8+ T cells were observed only at end-stage disease in mSOD1^{G93A}/CD4$^{-/-}$ mice (Fig. 2*D*).

Microglia From Mice Lacking T-Cells Are Not Dysfunctional. To ensure that the morphological reduction of microglia activation in mSOD1^{G93A}/RAG2$^{-/-}$ mice was not caused by an inherent dysfunction of the microglia, *in vitro* cultures of microglia from RAG2$^{-/-}$ mice were compared with microglia from WT mice for their ability to undergo morphological and functional activation. Following lipopolysaccharide (LPS) treatment, a treatment known to increase the release of tumor necrosis factor– α (TNF-α) and interleukin-1β (IL-1β), there were no differences in the production of TNF-α or IL-1β between microglia isolated from RAG2$^{-/-}$ mice compared with WT mice at any dose of LPS (Fig. S6*A* and *B*). Morphologically, there were also no differences between LPS-treated RAG2$^{-/-}$ microglia and LPS-treated WT microglia (data not shown). Thus, activated microglia from RAG2$^{-/-}$ mice are morphologically and functionally similar to activated WT microglia.

The Presence of CD4+ T-Cells Enhances Neuroprotection and Suppresses Cytotoxic Factors. mRNAs for the neurotrophic factors IGF-1 and GDNF were quantitatively decreased in the lumbar spinal cords of mSOD1^{G93A}/RAG2$^{-/-}$ mice compared with mSOD1^{G93A} and mSOD1^{G93A}/RAG2$^{+/-}$ mice and were similar to levels in WT mice (Fig. 4*C* and *D*). The mRNA for BDNF was decreased in both mSOD1^{G93A} and mSOD1^{G93A}/RAG2$^{+/-}$ mice but was further decreased in mSOD1^{G93A}/RAG2$^{-/-}$ mice (Fig. 4*E*). BMT of mSOD1^{G93A}/RAG2$^{-/-}$ mice with mSOD1^{G93A} donor-derived cells restored the levels of IGF-1, GDNF, and BDNF to those of mSOD1^{G93A}/RAG2$^{+/-}$ mice. Levels of these trophic factors were similar between mSOD1^{G93A}/RAG2$^{-/-}$ and mSOD1^{G93A}/CD4$^{-/-}$ mice. In contrast, the mRNA expression for NGF was not different between WT mice and any genotype of mSOD1^{G93A} mice in this study (Fig. S7*A*).

mRNA levels for several glutamate transporters, which are known to affect motoneuron viability, also paralleled survival (25, 26). Expression of GLT-1 and GLAST mRNAs was decreased in mSOD1^{G93A}/RAG2$^{-/-}$ and mSOD1^{G93A}/CD4$^{-/-}$ mice (Fig. 4*F* and *G*); GLAST mRNA levels were similar to levels in WT mice. BMT of mSOD1^{G93A}/RAG2$^{-/-}$ mice with mSOD1^{G93A} donor-derived cells restored the levels of GLT-1 and GLAST mRNA to those of mSOD1^{G93A}/RAG2$^{+/-}$ mice. EAAC1 mRNA levels were decreased in mSOD1^{G93A}, mSOD1^{G93A}/RAG2$^{+/-}$, mSOD1^{G93A}/RAG2$^{-/-}$, and mSOD1^{G93A}/CD4$^{-/-}$ mice compared with WT mice, and BMT of mSOD1^{G93A}/RAG2$^{-/-}$ mice did not alter EAAC1 levels in these mice (Fig. S7*B*).

The mRNA levels of IL-4 and TGF-β, two anti-inflammatory factors, were increased in mSOD1^{G93A} and mSOD1^{G93A}/RAG2$^{+/-}$ mice compared with WT mice (Fig. 4*H* and *I*) but were decreased in mSOD1^{G93A}/RAG2$^{-/-}$ and mSOD1^{G93A}/CD4$^{-/-}$ mice; BMT restored IL-4 and TGF-β levels to levels observed in mSOD1^{G93A} and mSOD1^{G93A}/RAG2$^{+/-}$ mice. The expression of Ym1 mRNA mirrored the IL-4 results across all genotypes of mSOD1^{G93A} mice, suggesting a loss of alternatively activated macrophages that are involved in resolving inflammation and promoting wound healing (Fig. S7*C*) (27). Fractalkine receptor (CX3CR1), expressed on microglia, monocytes, dendritic cells, and subsets of T cells, which has been shown to decrease microglial toxicity possibly by regulating the release of cytotoxic substances (28), was reduced in mSOD1^{G93A}/RAG2$^{-/-}$ and mSOD1^{G93A}/CD4$^{-/-}$ mice (Fig. S7*D*). BMT in mSOD1^{G93A}/RAG2$^{-/-}$ restored Ym1 and CX3CR1 mRNA to levels seen in mSOD1^{G93A} and mSOD1^{G93A}/RAG2$^{+/-}$ mice.

TNF-α mRNA levels were increased in mSOD1^{G93A} and mSOD1^{G93A}/RAG2$^{+/-}$ mice compared with WT mice, and were further elevated in mSOD1^{G93A}/RAG2$^{-/-}$ and mSOD1^{G93A}/CD4$^{-/-}$ mice (Fig. 4*J*). IL-6 was not increased in mSOD1^{G93A} or mSOD1^{G93A}/RAG2$^{+/-}$ mice compared with WT mice, but was increased in mSOD1^{G93A}/RAG2$^{-/-}$ mice (Fig. S7*E*). IL-6 expression was not elevated in mSOD1^{G93A}/CD4$^{-/-}$ mice, with levels similar to WT and mSOD1^{G93A} mice, possibly because of the presence of functional B cells in these mice. BMT reduced the TNF-α and IL-6 mRNA levels to those seen in mSOD1^{G93A} or mSOD1^{G93A}/RAG2$^{+/-}$ mice. TNF-α receptors I and II, iNOS, and IL-1β mRNA levels were not different in any of the genotypes of mSOD1^{G93A} mice studied (Fig. S7*F–I*).

The NADPH oxidase isoform NOX2 mRNA was elevated 70-fold in mSOD1^{G93A} and mSOD1^{G93A}/RAG2$^{+/-}$ mice compared with WT mice, and was increased 110-fold in mSOD1^{G93A}/RAG2$^{-/-}$ and mSOD1^{G93A}/CD4$^{-/-}$ mice (Fig. 4K). BMT in mSOD1^{G93A}/RAG2$^{-/-}$ mice reduced the NOX2 mRNA levels to those seen in mSOD1^{G93A} or mSOD1^{G93A}/RAG2$^{+/-}$ mice. The increased expression of proinflammatory cytokines and NOX2 does not lead to increased mouse or mutant human SOD1 mRNA expression, indicating that the shortened survival times are not caused by enhanced SOD1 mRNA expression (Fig. S7J and K) (29, 30).

Discussion

Immune dysfunction is a pathological feature in human ALS and mSOD1 transgenic mice (31). Because T cells are present at sites of motoneuron injury (9) and their role in injury is not known, this study directly addressed whether T cells contribute to the disease process of mSOD1^{G93A}-initiated chronic motoneuron degeneration. The results establish that the lack of T-cell recruitment, either through the loss of CCR2 or developmental inhibition, accelerates disease progression and the demise of these mice. These studies demonstrate for the first time that CD4+ T cells, directly or indirectly, are possibly the subpopulation of T cells that are neuroprotective in this model of inherited chronic neurodegeneration.

To determine whether recruitment of peripheral immune cells and/or microglia is essential for neuroprotection, mSOD1^{G93A}/PU.1$^{-/-}$ mice received BMT from CCR2$^{-/-}$ donor mice. Although onset of disease was not altered, disease progression was accelerated. In addition, these mice lacked CD3+ T cells and morphologically activated microglia, which were observed in mSOD1^{G93A}/PU.1$^{-/-}$ mice transplanted with mSOD1^{G93A} or WT bone marrow. Acceleration of disease after CCR2$^{-/-}$ BMT suggests that recruitment of microglia/monocytes and/or lymphocytes is involved in the pathogenesis of motoneuron injury, possibly by modulating glial function. A similar outcome was noted in a transgenic mouse model of Alzheimer disease, in which CCR2 deficiency accelerated disease progression and impaired microglial accumulation (18).

To dissociate the effects of microglia/myeloid cell recruitment from lymphocyte recruitment as mediators of disease progression, mSOD1^{G93A}/RAG2$^{-/-}$ mice were developed. Although disease onset was not altered, the lack of functional lymphocytes accelerated disease progression in mSOD1^{G93A}/RAG2$^{-/-}$ mice. These data demonstrate, in a chronic neurodegenerative disease model, that lymphocytes are possibly needed for neuroprotection and microglial morphological activation. Although two recent reports suggest that 1100 cGy γ-irradiation dose may artificially induce circulating myeloid cells to infiltrate the CNS (21, 22), following a sublethal 400-cGy dose, spinal cord sections from mSOD1^{G93A}/RAG2$^{-/-}$ mice transplanted with GFP+ donor-derived bone marrow contained only GFP+ lymphocytes; no GFP+ cells with myeloid cell morphologies were present (data not shown). Furthermore, these previous studies did not report on the recruitment or infiltration of T cells into the CNS after lethal γ-irradiation treatment. In this study, the composition of T-cell subpopulations was similar between mSOD1^{G93A}/RAG2$^{+/-}$ mice and γ-irradiated mSOD1^{G93A}/RAG2$^{-/-}$ mice after BMT; the number and subtypes of T cells was not altered because of γ-irradiation treatment. Nevertheless, to rule out the possibility that irradiation, myeloid cells, or other leukocytes influenced disease onset, survival, or duration, mSOD1^{G93A}/RAG2$^{-/-}$ mice were transplanted with RAG2$^{-/-}$ derived bone marrow, and no beneficial effects were noted. In addition, WT and mSOD1^{G93A} bone marrow cells have equivalent neuroprotective abilities to prolong survival, possibly by modulating glial function. A possible explanation for these equivalent effects is that the donor-derived bone marrow precursor T cells are "educated" by the recipient's own local immune environment and, regardless of the T-cell genotype, the host will direct the activation of these transplanted lymphocytes.

Because CD4+ T cells were observed in the spinal cord during all phases of disease, including disease onset and during the plateau phase, and CD8+ T cells were present only in the terminal stages, CD4+ T cells may represent the relevant neuroprotective subpopulation of lymphocytes that prolonged survival in transplanted mSOD1^{G93A}/RAG2$^{-/-}$ mice. To test this hypothesis, mSOD1^{G93A}/CD4$^{-/-}$ mice were generated and compared with their mSOD1^{G93A}/CD4$^{+/-}$ littermates, and although disease onset was not altered, disease progression in mSOD1^{G93A}/CD4$^{-/-}$ mice was accelerated to the same extent as in mSOD1^{G93A}/RAG2$^{-/-}$ mice. Thus, the CD4+ T cells that entered the spinal cord at sites of motoneuron injury appear to be neuroprotective (12, 14, 16), whereas the CD8+ T cells present at end-stage disease are possibly associated with injury.

In mSOD1^{G93A}/RAG2$^{+/-}$ and BMT mSOD1^{G93A}/RAG2$^{-/-}$ mice, the T cells were localized throughout the ventral gray matter. Although 5 to 10 T cells per section were observed in mSOD1^{G93A}/RAG2$^{+/-}$ mice between the disease onset and the plateau phase of disease progression, which later increased to 19 T cells per section, similar numbers and subtypes of T cells were observed in mSOD1^{G93A}/RAG2$^{-/-}$ mice following BMT with either mSOD1^{G93A} or WT donor-derived cells. In contrast, although T cells are known to be present in the central nervous system of mice under normal conditions, their presence is a rare event. Thus, as has been previously reported (32), even at these earlier time points, the documented presence of T cells may have a considerable impact on the area's local immune response and may alter the trophic versus toxic balance of glia in these areas of chronic CNS neurodegeneration. However, it is also possible that the neuroprotective benefits of T-lymphocytes may be amplified by their presence at the neuromuscular junction or contiguous with injured motoneuron axons.

CD4+ T cells have also been reported to influence survival in an acute facial motoneuron injury model, possibly related to CD4+ secretion of BDNF (12). In that model, CD4+ T-cell–mediated neuroprotection was found to depend on both resident microglia and peripherally derived antigen-presenting cells (15). The activation of microglia, which causes them to function as antigen-presenting cells and to express MHC class II proteins, is correlated with a better outcome following CNS injury (11). Thus, the beneficial or destructive outcome of the local microglial response is determined by a well-controlled dialog between the innate and adaptive immune systems; and, under specific circumstances and with the correct stimulation, T cells are anti-inflammatory and protect motoneurons from degenerating. Furthermore, in conjunction with previous BMT data (6), the CCR2$^{-/-}$ BMT and RAG2$^{-/-}$ data suggest that disease progression is influenced by lymphocytes as well as by glia (5–7). Most significantly, these data indicate that CD4+ T cells, either directly or indirectly, are the subpopulation of T cells that may be responsible for prolonging survival in this model of neurodegeneration.

The activation states of microglia and astrocytes, with respect to protection versus toxicity, cannot be inferred solely from their morphologies. The conventional morphological markers for activation were attenuated in mSOD1^{G93A}/RAG2$^{-/-}$ and mSOD1^{G93A}/CD4$^{-/-}$ mice; yet the mRNA for NOX2, which is known to enhance microglial release of reactive oxygen species (33), was elevated and contributed to more rapid disease progression and death. Thus, morphological (CD11b, CD68, GFAP) markers of glial "activation" do not accurately predict the functional (TNF-α, NOX2) markers of "activation." The apparent morphological reduction of microglial activation occurs early in disease, indicating that the presence of T cells may increase the morphological activation state and antigen presentation abilities of microglia and may contribute to increased survival. Although not different at end stage, these results also suggest that all glial responses are not attenuated and that an increased astroglial response at earlier time points is neuroprotective. Furthermore, the data suggest that
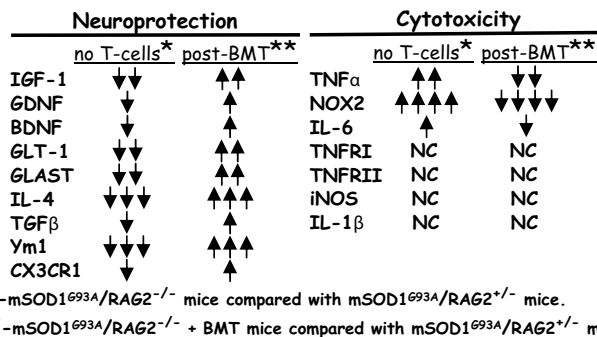
Neuroprotection			Cytotoxicity		
	no T-cells*	post-BMT**		no T-cells*	post-BMT**
IGF-1	↓↓	↑↑	TNFα	↑↑	↓↓
GDNF	↓	↑↑	NOX2	↑↑↑↑	↓↓↓
BDNF	↓↓	↑↑	IL-6	↑↑	↓↓
GLT-1	↓↓	↑↑	TNFRI	NC	NC
GLAST	↓↓	↑↑	TNFRII	NC	NC
IL-4	↓↓↓	↑↑↑	iNOS	NC	NC
TGFβ	↓	↑↑↑	IL-1β	NC	NC
Ym1	↓	↑↑			
CX3CR1	↓↓↓	↑↑			

*-mSOD1^{G93A}/RAG2$^{-/-}$ mice compared with mSOD1^{G93A}/RAG2$^{+/-}$ mice.

**-mSOD1^{G93A}/RAG2$^{-/-}$ + BMT mice compared with mSOD1^{G93A}/RAG2$^{+/-}$ mice.

Fig. 5. The presence of T cells shifts the balance of microglial and astroglial responses from reduced protection and increased cytotoxicity to increased neuroprotection and decreased toxicity following BMT. ↓↓↓ >75% decrease; ↓↓ 50–75% decrease; ↓, 0–50% decrease; NC, no change; ↑, 100–500% increase; ↑↑, 600–1500% increase; and ↑↑↑, 1600–2500% increase; ↑↑↑↑, 2600–5000% increase.

disease progression may be influenced by lymphocytes indirectly or possibly even directly, interacting with glia, balancing the trophic versus cytotoxic responses of microglia and astroglia. CD4+ T cells should now be included in the non–cell-autonomous hypothesis of neuroprotection (1).

The shortened length of survival in mSOD1^{G93A}/RAG2$^{-/-}$ and mSOD1^{G93A}/CD4$^{-/-}$ mice is partly due to decreased levels of neurotrophic factors and the reduced abilities of glia to remove glutamate, thus enhancing motoneuron excitotoxicity. Not only are neurotrophic and anti-inflammatory factors reduced in mSOD1^{G93A}/RAG2$^{-/-}$ and mSOD1^{G93A}/CD4$^{-/-}$ mice, the messages for TNF-α and superoxide are increased, suggesting a decrease of protective factors and an increase in toxic molecules (Fig. 5). More importantly, BMT reconstituted mice with functional T cells and restored the neuroprotective factors, and also decreased the toxic and proinflammatory responses. These results suggest that CD4+ T cells directly or indirectly provide neuroprotection by modulating the trophic/cytotoxic balance of glia. Expanding this

population may offer further protection in diverse forms of dominantly inherited chronic neurodegenerative diseases and may provide a novel target for critically needed therapies.

Materials and Methods

mSOD1^{G93A}, PU.1, RAG2, and CD4 Mice. All animal protocols were approved by the Methodist Research Institute's Institutional Animal Care and Use Committee in compliance with National Institutes of Health guidelines. Housing, breeding, and screening details are found in *SI Methods*.

Bone Marrow Transplantation. Donor bone marrow was obtained from 9 to 12 weeks old WT, mSOD1^{G93A}, or CCR2$^{-/-}$ mice, and transplanted into the mSOD1^{G93A}/PU.1$^{-/-}$ pups within 24 h of birth as previously described (6). mSOD1^{G93A}/RAG2$^{-/-}$ mice were sublethally γ-irradiated (400 rads) and transplanted with WT, mSOD1^{G93A}, or RAG2$^{-/-}$ donor-derived bone marrow. Details are provided in *SI Methods*.

Quantitative RT-PCR. RNA was isolated and purified from lumbar spinal cords, and quantitative RT-PCR was performed as previously described (19). Technical details are given in *SI Methods*.

Immunohistochemistry and Antibodies. Spinal cord tissue was evaluated for the expression of CD3, CD4, CD8, CD11b, CD11c, CD19, CD40, CD68, MCH class II, and GFAP. Technical details are found in *SI Methods*.

Primary Microglia Cultures. Primary microglial cultures were prepared from 8- to 9-day-old mice and treated with LPS as previously described (6). Details are given in *SI Methods*.

Statistical Analyses. Data were analyzed using two-tailed Student's *t* test using Excel (Microsoft software). Data are expressed as mean± SEM; $P < 0.05$ was considered statistically significant. Differences in onset and survival times were computed using Kaplan–Meier survival statistics (log-rank-sum test; Number Cruncher Statistical Systems, Kaysville, UT). Disease progression and the *in vitro* studies were analyzed using a one-way analysis of variance (ANOVA) with repeated measures (SigmaStat, Richmond CA). Differences between groups were analyzed using a two-way ANOVA (SigmaStat).

1. Lobsiger CS, Cleveland DW (2007) Glial cells as intrinsic components of non-cell-autonomous neurodegenerative disease. *Nat Neurosci* 10:1355–1360.
2. Rowland LP, Shneider NA (2001) Amyotrophic lateral sclerosis. *N Engl J Med* 344:1688–1700.
3. Gurney M, *et al.* (1994) Motor neuron degeneration in mice that express a human Cu,Zn superoxide dismutase mutation. *Science* 264:1772–1775.
4. Boillée S, Vande Velde C, Cleveland DW (2006) ALS: A disease of motor neurons and their nonneuronal neighbors. *Neuron* 52:39–59.
5. Yamanaka K, *et al.* (2008) Astrocytes as determinants of disease progression in inherited amyotrophic lateral sclerosis. *Nat Neurosci* 11:251–253.
6. Beers DR, *et al.* (2006) Wild-type microglia extend survival in PU 1 knockout mice with familial amyotrophic lateral sclerosis. *Proc Natl Acad Sci USA* 103:16021–16026.
7. Boillée S (2006) *et al.* Onset and progression in inherited ALS determined by motor neurons and microglia. *Science* 312:1389–1392.
8. Wyss-Coray T, Mucke L (2002) Inflammation in neurodegenerative disease—a double-edged sword. *Neuron* 35:419–432.
9. Alexianu ME, Kozovska M, Appel SH (2001) Immune reactivity in a mouse model of familial ALS correlates with disease progression. *Neurology* 57:1282–1289.
10. Ghasemlou N, Jeong SY, Lacroix S, David S (2007) T cells contribute to lysophosphatidylcholine-induced macrophage activation and demyelination in the CNS. *Glia* 55:294–302.
11. Schwartz M, Butovsky O, Brück W, Hanisch UK (2006) Microglial phenotype: Is the commitment reversible? *Trends Neurosci* 29:68–74.
12. Serpe CJ, Byram SC, Sanders VM, Jones KJ (2005) Brain-derived neurotrophic factor supports facial motoneuron survival after facial nerve transaction in immunodeficient mice. *Brain Behav Immun* 19:173–80.
13. Schwartz M, Kipnis J (2005) Therapeutic T cell-based vaccination for neurodegenerative disorders: The role of CD4+CD25+ regulatory T cells. *Ann NY Acad Sci* 1051:701–708.
14. Kipnis J, Schwartz M (2005) Controlled autoimmunity in CNS maintenance and repair: Naturally occurring CD4+CD25+ regulatory T cells at the crossroads of health and disease. *Neuromol Med* 7:197–206.
15. Byram SC, *et al.* (2004) CD4-positive T cell-mediated neuroprotection requires dual compartment antigen presentation. J Neurosci 24:4333–4339.
16. Serpe CJ, Coers S, Sanders VM, Jones KJ (2003) CD4+ T, but not CD8+ or B, lymphocytes mediate facial motoneuron survival after facial nerve transaction. *Brain Behav Immun* 17:393–402.
17. Babcock AA, Kuziel WA, Rivest S, Owens T (2003) Chemokine expression by glial cells directs leukocytes to sites of axonal injury in the CNS. *J Neurosci* 23:7922–7930.
18. El Khoury J, *et al.* (2007) Ccr2 deficiency impairs microglial accumulation and accelerates progression of Alzheimer-like disease. *Nat Med* 13:432–438.
19. Henkel JS, Beers DR, Siklos L, Appel SH (2006) The chemokine MCP-1 and the dendritic and myeloid cells it attracts are increased in the mSOD1 mouse model of ALS. *Mol Cell Neurosci* 31:427–437.
20. Shinkai Y, *et al.* (1992) RAG-2-deficient mice lack mature lymphocytes owing to inability to initiate V(D)J rearrangement. *Cell* 68:855–867.
21. Ajami B, Bennett JL, Krieger C, Tetzlaff W, Rossi FM (2007) Local self-renewal can sustain CNS microglia maintenance and function throughout adult life. *Nat Neurosci* 10:1538–1543.
22. Mildner A, *et al.* (2007) Microglia in the adult brain arise from Ly-6ChiCCR2+ monocytes only under defined host conditions. *Nat Neurosci* 10:1544–1553.
23. Petri S, Kiaei M, Wille E, Calingasan NY, Beal FM (2006) Loss of Fas ligand-function improves survival in G93A-transgenic ALS mice. *J Neurol Sci* 251:44–49.
24. Rahemtulla A, *et al.* (1991) Normal development and function of CD8+ cells but markedly decreased helper cell activity in mice lacking CD4. *Nature* 353:180–184.
25. Regan MR, *et al.* (2007) Variations in promoter activity reveal a differential expression and physiology of glutamate transporters by glia in the developing and mature CNS. *J Neurosci* 27:6607–6619.
26. Sheldon AL, Robinson MB (2007) The role of glutamate transporters in neurodegenerative diseases and potential opportunities for intervention. *Neurochem Int* 51:333–355.
27. Ponomarev ED, Maresz K, Tan Y, Dittel BN (2007) CNS-derived interleukin-4 is essential for the regulation of autoimmune inflammation and induces a state of alternative activation in microglial cells. *J Neurosci* 27:10714–10721.
28. Cardona AE, *et al.* (2006) Control of microglial neurotoxicity by the fractalkine receptor. *Nat Neurosci* 9:917–924.
29. Marikovsky M, Ziv V, Nevo N, Harris-Cerruti C, Mahler O (2003) Cu/Zn superoxide dismutase plays important role in immune response. *J Immunol* 170:2993–3001.
30. Nguyen MD, D'Aigle T, Gowing G, Julien J-P, Rivest S (2004) Exacerbation of motor neuron disease by chronic stimulation of innate immunity in a mouse model of amyotrophic lateral sclerosis. *J Neurosci* 24:1340–1349.
31. McGeer PL, McGeer EG (2002) Inflammatory processes in amyotrophic lateral sclerosis. *Muscle Nerve* 26:459–470.
32. Steinman L (1996) A few autoreactive cells in an autoimmune infiltrate control a vast population of nonspecific cells: A tale of smart bombs and the infantry. *Proc Natl Acad Sci USA* 93:2253–2256.
33. Harraz MM, *et al.* (2008) SOD1 mutations disrupt redox-sensitive Rac regulation of NADPH oxidase in a familial ALS model. *J Clin Invest* 118:659–670.

NEUROSCIENCE